Effective and Interpretable Information Aggregation with Capacity Networks

Markus Zopf

NEC Laboratories Europe
Heidelberg, Germany
markus.zopf@neclab.eu

Abstract

How to aggregate information from multiple instances is a key question multiple instance learning. Prior neural models implement different variants of the well-known encoder-decoder strategy according to which all input features are encoded a single, high-dimensional embedding which is then decoded to generate an output. In this work, inspired by Choquet capacities, we propose Capacity networks. Unlike encoder-decoders, Capacity networks generate multiple interpretable intermediate results which can be aggregated in a semantically meaningful space to obtain the final output. Our experiments show that implementing this simple inductive bias leads to improvements over different encoder-decoder architectures in a wide range of experiments. Moreover, the interpretable intermediate results make Capacity networks interpretable by design, which allows a semantically meaningful inspection, evaluation, and regularization of the network internals.

Introduction

In many important problems, a label is not given for each individual instance but only a set of instances. For instance, in histopathological classification of breast cancer images (Sudharshana et al. 2019), only one label that indicates if a patient has cancer or not is given for a set of images. Similarly, in drug activity prediction (Dietterich, Lathrop, and Lozano-Pérez 1997), a label is only provided for a set of molecule shapes, but not for individual molecule shapes. In sentiment analysis, only a single label may be given for a document that is comprised of multiple sentences, without labeling information on the sentence level (Pappas and Popescu-Belis 2017; McAuley, Leskovec, and Jurafsky 2012).

Problems with this characteristic are in the focus of *multiple instance learning* (MIL) (Dietterich, Lathrop, and Lozano-Pérez 1997; Maron and Lozano-Perez 1998; Ray and Page 2001; Carbonneau et al. 2018). More formally, in MIL, an input consists of a set of instances $X \subset \mathcal{G}$, where $\mathcal{G}$ is a ground set of individual instances. The goal is to learn a set function f from training pairs (X_i, Y_i) that maps input sets to set labels. Supervision (i.e. labeling information) for individual instances is not provided.

A key question in MIL is how to aggregate the information from the multiple instances in the input sets. Prior neural approaches for MIL such as Zaheer et al. (2017); Ilse, Tomczak, and Welling (2018); Murphy et al. (2019); Lee et al. (2019) implement different variants of the encoder-decoder strategy. Encoder-decoders use an encoder networks to aggregate the features of all individual instances $x_1, \ldots, x_n \in X$ into a single, high-dimensional set embedding Z. The set embedding is then decoded by a decoder network to generate an output Y. We provide a high-level illustration of sequential and parallel encoder-decoder networks in Figure 1a.

In this work, we present an alternative approach to aggregate information from multiple instances and demonstrate its effectiveness and interpretability. Inspired by a sequential decomposition of Choquet capacities (Choquet 1954; Sugeno 1974), we propose to decompose multiple instance learning tasks with sets of size n into n smaller sub-problems (i.e. one for each instance in the input) and to produce a meaningful intermediate result for each sub-problem. More specifically, for each instance i, an neural module generates an intermediate set embedding which is immediately decoded by another neural module to generate an intermediate result. Each intermediate result models the added value of instance x_i with respect to all already seen instances $x_1, \ldots, x_{i-1}$. Like in Choquet capacities, all intermediate results can be simply summed to obtain the final output. In Figure 1, we illustrate the architectures of the resulting family of neural networks, which we denote as Capacity networks, and show how it differs from encoder-decoder architectures.

Capacity networks have two major advantages over their encoder-decoder counterparts: *improved effectiveness* and *interpretability by design*. More specifically, we find that Capacity networks achieve better results than prior works in a wide range of experiments. A potential explanation for the improved performance is that Capacity networks are better able to leverage the compositional nature of MIL problems. Moreover, Capacity networks are interpretable by design. Prior encoder-decoder architectures are end-to-end black boxes. In contrast, Capacity network generate multiple meaningful intermediate results that can easily be interpreted. The improved interpretability allows to evaluate if the trained models are right for the right reasons. Moreover, a quantitative evaluation of the intermediate results is pos-

(a) Parallel and sequential encoder-decoder networks

(b) Capacity networks
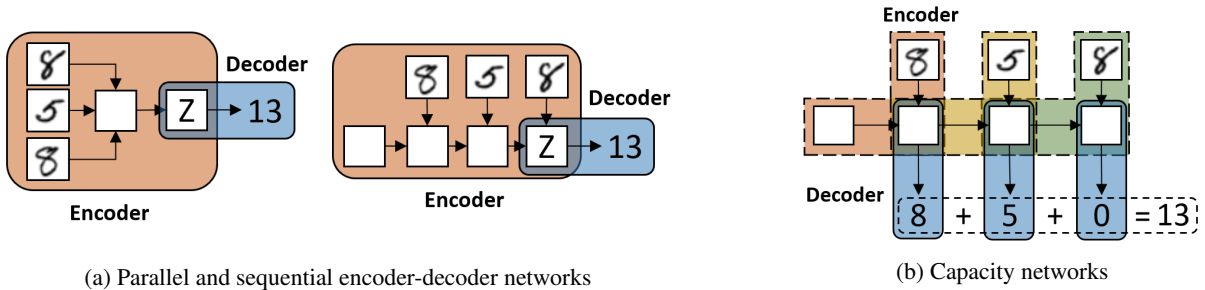
Figure 1: High-level illustration of parallel and sequential encoder-decoders (1a) and the newly proposed Capacity networks (1b) applied to an instance of a popular MNIST-based multiple instance regression problem called 'unique sum' (Murphy et al. 2019; Kalra et al. 2020). The input consists of a set of MNIST images (in this example the three images 8, 5, and 8) and the output equals to the sum of uniquely appearing MNIST images. Both encoder-decoder architectures generate a set embedding Z which is decoded to obtain the output and, hence, serves as interface between encoder and decoder. In contrast, Capacity networks apply a decoder three times to generate three intermediate results, each of which modeling the added value of instance x_i with respect to all already observed instances $x_1, \ldots, x_{i-1}$. We use red, yellow, and green to illustrate that the encoder network is applied three times.

sible. Furthermore, the intermediate results allow to inject semantically meaningful prior knowledge into the training process via regularization terms. To summarize, our contributions are as follows:

1. We propose Capacity networks that implement an alternative information aggregation strategy for multiple instance learning. Our key idea is to generate an interpretable, scalar-valued intermediate result for each instance that represents its added value with respect to all already observed instances and to sum all generated intermediate results to obtain the final prediction.

2. We show that Capacity networks are more effective than prior encoder-decoder architectures at learning challenging set functions. Moreover, we show that Capacity networks perform better for large sets, for varying set sizes, with smaller amounts of training data, and in a real-world sentiment analysis dataset.

3. We demonstrate the interpretability of Capacity networks, which enable a quantitative evaluation of the network internals and the implementation of a semantically meaningful regularization.

Capacity Networks

In the following, we discuss an iterative decomposition of Choquet capacities, which motivate the fundamental architecture of Capacity networks.

Iterative Decomposition of Choquet Capacities

Let $\mathcal{G} = \{x_1, \ldots, x_m\}$ be a set of instances. A set function $\mu : \mathcal{P}(\mathcal{G}) \to [0, \infty)$ is called *(Choquet) capacity* (Choquet 1954; Sugeno 1974) if $\mu(\emptyset) = 0$ and $\mu(A) \le \mu(B)$ for $A \subseteq B \subseteq \mathcal{G}$. Unlike measures such as the Lebesgue measure, capacities are not additive, which is essential to model non-additive aggregation effects, i.e. problems where $\mu(A \cup B) = \mu(A) + \mu(B), \forall A, B \in \mathcal{G}$ with $A \cap B = \emptyset$ does not hold in general. A capacity μ is called *superad-*

ditive if $\mu(A \cup B) \ge \mu(A) + \mu(B)$ and *subadditive* if $\mu(A \cup B) \le \mu(A) + \mu(B)$, for $A \cap B = \emptyset, A, B \in \mathcal{P}(\mathcal{G})$.

Given a capacity μ, it is natural to ask how large the individual contribution of a single instance x_i is to a set $X = \{x_1, \ldots, x_n\}, x_i \notin X$. More formally: Given $X \subset \mathcal{G}, x_i \notin X$, how large is $\mu(X \cup \{x_i\}) - \mu(X)$? In the additive case (like in measures), the difference always equals to $\mu(\{x_i\})$. However, in the non-additive case, the added value of x_i to X depends on X. The motivation to identify the individual contribution of an instance to a set utility naturally leads to the following sequential decomposition:

$$
\begin{aligned}
\mu(X) = \quad & [\mu(\emptyset \cup \{x_1\}) - \mu(\emptyset)] \\
& + [\mu(\{x_1\} \cup \{x_2\}) - \mu(\{x_1\})] \\
& + \ldots \\
& + [\mu((X) - \mu(X \setminus \{x_n\})].
\end{aligned}
\tag{1}
$$

Each row in Equation 1 represents the *added value* of a single instance with respect to all previous instances. Equation 1 can be summarized as

$$
\mu(X) = \sum_{i=1}^{|X|} \nu_i, \text{ with } \nu_i = \mu(C_{i-1} \cup \{x_i\}) - \mu(C_{i-1}), \tag{2}
$$

where $C_{i-1} = \{x_1, \ldots, x_{i-1}\}$, and $C_0 = \emptyset$. The first summand $\nu_1 = \mu(C_0 \cup \{x_1\}) - \mu(C_0)$ equals $\mu(\{x_1\}))$. In other words, ν_1 represents the intrinsic value of x_1. Similarly, we obtain $\mu(\{x_1, x_2\}) - \mu(\{x_1\})$ for ν_2 which can be interpreted as estimating the added value of x_2 with respect to x_1. Finally, ν_n equals to the added value of the last instance x_n with respect to all other instances $x_1, \ldots, x_{n-1}$. The decomposition requires an ordering of the instances in X. Otherwise, it is unclear which instance should be considered first, second, etc. To this end, any arbitrary total ordering can be used. The input in Figure 1, $X = \{8, 5, 8\}$),

can, for instance, be decomposed as

$$\mu(X) = \mu(\{ 8 \})$$
$$+ [\mu(\{ 8, 5 \}) - \mu(\{ 8 \})] \quad (3)$$
$$+ [\mu(\{ 8, 5, 8 \}) - \mu(\{ 8, 5 \})].$$

According to this decomposition and the 'unique sum' task described in Figure 1, we first compute the individual contribution of image 8 (which is 8), then we compute the contribution of the next image 5 with respect to the already considered image 8 (which is 5), and finally compute the contribution of last image 8 with respect to 8 and 5 (which is 0, since class '8' has already appeared once).

Network Architecture

Inspired by the sequential decomposition of capacities, we now define a new family of neural networks for multiple instance learning. Key idea is to introduce an inductive bias such that neural networks mimic the discussed sequential decomposition of capacities. To this end, we propose to design networks such that they generate an intermediate result y_i after reading instance x_i which models the added value of instance x_i to the set of all already seen instances $\{x_1, \ldots, x_{i-1}\}$. As in Equation 2, the output of the network for a set X can be obtained by simply computing the sum of all intermediate results. In terms of encoder and decoder functions, we define Capacity networks as

$$z_i = \text{encoder}(x_i, z_{i-1}) \quad (4)$$
$$y_i = \text{abs}(\text{decoder}(z_i)) \quad (5)$$
$$Y = \sum_{i=1}^{|X|} y_i, \quad (6)$$

where z_0 is an initial state and abs(.) denotes the absolute value of the decoder output. We compute abs(.) to model the fact that each $\nu_i \geq 0$, since $\mu(C_{i-1} \cup \{x_i\}) \geq \mu(C_{i-1})$ due to the monotonicity of μ. In principal, this additional inductive bias is not essential for the networks architecture and can be removed if monotonicity should not be enforced. Furthermore, we do not explicitly model subtrahend and minuend explicitly but estimate the difference directly. Again, this is a non-essential design choice that can be modified in future work.

Capacity networks are closely connected the sequential decomposition of capacities presented in Equation 2. Each application of the decoder in Equation 5 corresponds to one ν_i in Equation 2, which represents the added value of the i-th instance with respect to all already observed instances. Similar to the sequential decomposition of capacities in Equation 2, Capacity networks require a sequential ordering of the inputs. Otherwise, it is not possible to model the added value of an instance with respect to already seen instances. Any sequential network such as RNNs, LSTMs, and GRUs can be used as basis to implement the proposed inductive bias. Hence, we do not present a specific neural networks but rather a new family of neural networks. Capacity networks

are not guaranteed to be permutation invariant. This is, however, not necessarily a limitation of the presented idea. Sequential approaches have been demonstrated to show strong performance for MIL in prior works. Furthermore, several methods exist to mitigate or completely remove the permutation sensitivity of permutation sensitive networks as described in the next section. Permutation sensitivity can even be viewed as advantage since our networks can also be used if the output depends on the order of the input instances (e.g. in ordered sets or sequences).

A key distinction between prior encoder-decoder architectures and the newly presented idea is that encoder-decoders do not produce intermediate results, whereas Capacity networks generate n intermediate results, each of which modeling the added value of a specific instance. Another way to describe this distinction is to note that standard encoder-decoders only produce a single latent set embedding which is fed only once into a decoder to produce a scalar-valued output. In contrast, Capacity networks apply a decoder several times (once for each produced latent state z_i) to produce many latent scalar-valued intermediate results. As a consequence, encoder-decoders aggregate information from different instances in an uninterpretable high-dimensional feature space, whereas Capacity networks aggregate interpretable scalar-valued intermediate results. The inductive bias to generate scalar-valued intermediate results can also be viewed as introducing multiple information bottlenecks into the network architectures since the Capacity networks need to compress the feature representation to a meaningful, one-dimensional value multiple times.

Related Work

Capacities and Choquet integration have already inspired other works in machine learning before. Beliakov (2008) fit values of the discrete Choquet integral with linear programming techniques. Tehrani et al. (2012) use the Choquet integral to model monotone nonlinear aggregations for binary classification. Tehrani, Cheng, and Hullermeier (2012) use the Choquet integral in a pairwise preference learning scenario. Dias et al. (2018) replace pooling layers in convolutional neural networks with Choquet integration. In contrast to our work, they consider a classification setup and do not consider multiple instance learning. Karczmarek, Kiersztyn, and Pedrycz (2018) and Karczmarek, Kiersztyn, and Pedrycz (2019) use the Choquet integral to build an ensemble of classifiers for face recognition. Similarly, Anderson et al. (2018) and Scott et al. (2017) build an ensemble of CNNs.

Many works on multiple instance classification (Dietterich, Lathrop, and Lozano-Pérez 1997; Maron and Lozano-Perez 1998) and regression (Ray and Page 2001; Herbrich, Minka, and Graepel 2006) make strong task-specific assumption (Carbonneau et al. 2018). For instance, Dietterich, Lathrop, and Lozano-Pérez (1997) assume that the label of a set is positive if at least one instance in the set is positive (commonly known as the standard MIL assumption (Carbonneau et al. 2018)). Similarly, Ray and Page (2001) assume that the target variable depends only on a single primary instance. TrueSkill (Herbrich, Minka, and

Graepel 2006) assumes additivity. These independence assumptions simplify the problem substantially, since models do not have to consider interdependencies between instances. In contrast, we consider more challenging non-additive problems. Prior neural approaches for MIL such as Zaheer et al. (2017); Ilse, Tomczak, and Welling (2018); Murphy et al. (2019); Kalra et al. (2020) implement different variants of the encoder-decoder strategy. The approaches can be grouped into two groups, depending on whether the encoder network reads all input instances in parallel or sequentially (see Figure 1a).

Parallel architectures usually use a permutation invariant pooling operation such as sum, mean, or max to generate a set embedding (Lee et al. 2019). Zaheer et al. (2017) show that permutation invariant architectures can be described in a fairly simple framework consisting of a network ϕ that maps instance into a latent feature space, a sum pooling operation, and a decoder network ρ. In this case, the encoder can be written as $\text{encoder}(X) = \sum_{x \in X} \phi(x) = Z$ and the decoder is simply $\text{decoder}(Z) = \rho(Z)$. Even though using a sum is sufficiently expressive from a theoretical point of view, Soelch et al. (2019) show that the networks can be highly sensitive to the choice of the aggregation function in practice. Similarly, PointNets (Qi et al. 2017) and PointNetST (Segol and Lipman 2020) are universal approximations of invariant and equivariant set functions, respectively. Soelch et al. (2019) propose a trainable recurrent aggregation function based on the read-process-write architecture (Vinyals, Bengio, and Kudlur 2016). Similarly, Ilse, Tomczak, and Welling (2018) and Yang et al. (2020) use an attention-based weighted aggregation. The encoder can be written as $\text{encoder}(X) = \sum_{x \in X} a_i \cdot \phi(x_i)$ where $a_i = \frac{\exp h(x_i)}{\sum_{j=1}^{|X|} \exp h(x_j)}$ and h is an implementation-specific function to transform the input features. Lee et al. (2019) present the self-attention-based (Vaswani et al. 2017) Set Transformer and describe how their architecture fits into the encoder-decoder design pattern. Similarly, Deep Message Passing on Sets (Shi, Oliva, and Niethammer 2020) can also model interactions between different instances.

Sequential architectures generate the embedding Z with a sequential encoder network. For instance, Vinyals, Bengio, and Kudlur (2016) compute attention weights based on the hidden state of an LSTM and the input instances. Hence, the encoder can be formulated as $\text{encoder}(X) = \sum a_i x_i$, where a_i are the last layer's attention weights. Since sequential encoder-decoders consume one instance at each timestep t (Cho et al. 2014; Luong, Pham, and Manning 2015), the output may change when the input is permuted (Vinyals, Bengio, and Kudlur 2016). Several approaches exist to use permutation-sensitive models as basis for creating permutation-invariant models. A very simple yet effective approach is to order the objects in the input set according to an arbitrary total ordering π before they are fed into the permutation-sensitive model (Niepert, Ahmed, and Kutzkov 2016). Zhang, Hare, and Prügel-Bennett (2020) present a pooling method for sets of feature vectors which can be used to construct permutation-equivariant models. Janossy pooling (Murphy et al. 2019) aggregates the outputs of per-

	UC	US	WTri	US+S	TriC	Sent
RNN	0.56	0.91	1.73	6.76	4.09	1.98
LSTM	0.22	0.43	0.87	2.68	**1.01**	1.58
GRU	0.21	0.47	0.86	2.44	3.02	0.74
$\mathcal{C}$-RNN (ours)	0.22	0.43	0.57	2.57	3.17	0.70
$\mathcal{C}$-LSTM (ours)	0.25	0.27	0.59	**1.61**	1.02	**0.67**
$\mathcal{C}$-GRU (ours)	**0.18**	**0.25**	**0.48**	1.63	2.13	0.71
DeepSet	0.51	0.27	2.90	2.19	2.03	0.79
Attention	0.73	0.51	1.01	2.44	3.12	1.98
Set Trans.	0.30	1.91	8.72	14.74	1.22	0.92
Set Trans. L	0.28	1.72	3.01	12.61	1.19	0.91

Table 1: Mean squared errors of three different runs for different architectures in the multiple instance learning datasets. Median results and standard deviation can be found in the supplementary material.

mutation sensitive models to obtain a permutation-invariant model or an approximation thereof. Meng et al. (2019) extend Janossy pooling and use an LSTM to construct a hierarchical feature aggregation network for set-of-sets problems. Zhang, Prügel-Bennett, and Hare (2019) learn how to order the instances in sets before they are fed into an LSTM. Similarly, Mena et al. (2018) learn to reconstruct scrambled objects with Gumbel-Sinkhorn networks. Neural networks with external memories (Das, Giles, and Sun 1992; Schmidhuber 1992, 1993) such as RNNSearch (Bahdanau, Cho, and Bengio 2015), Memory Networks (Weston, Chopra, and Bordes 2015), and Neural Turing Machines (Graves, Wayne, and Danihelka 2014) are alternative permutation sensitive approaches. Similarly, AMRL (Beck et al. 2020) is an permutation invariant external memory for reinforcement learning. Unlike the intermediate results in Capacity networks, the external memory is an uninterpretable accumulator of knowledge.

Effectiveness Evaluation

In the following, we evaluate the effectiveness of Capacity networks and compare it with their non-capacity counterparts and other prior architectures. To this end, we implement three Capacity networks based on RNNs, LSTMs (Hochreiter and Schmidhuber 1997), and GRUs (Cho et al. 2014). We refer to the resulting Capacity networks as $\mathcal{C}$-RNN, $\mathcal{C}$-LSTM, and $\mathcal{C}$-GRU, respectively. Capacity networks have the same number of trainable parameters as their non-capacity counterparts. Following Zaheer et al. (2017), we use 3 fully connected layers for decoder and encoder. In all experiments, we feed the instances in random order into the networks. Additionally, we use a DeepSet (Zaheer et al. 2017), two Set Tranformers (Lee et al. 2019) with different sizes[1] and an attention-based network (Luong, Pham, and Manning 2015) as additional reference models. Mean squared error (MSE) is used as loss and evaluation metric. In all experiments, we report the average of three runs with dif-

---

[1] We use the code provided by the authors (Lee et al. 2019) at github.com/juho-lee/set_transformer.

ferent random seeds. Adam (Kingma and Ba 2015) is used as optimizer as it has been used by prior works (Murphy et al. 2019) and shows good performance across several tasks and setups (Schmidt, Schneider, and Hennig 2020). We perform the same hyperparameter optimization for all models. Additional details can be found in the supplementary material.

Datasets

We follow prior works (Zaheer et al. 2017; Ilse, Tomczak, and Welling 2018; Murphy et al. 2019; Kalra et al. 2020) and generate input sets X_i and corresponding labels Y_i based on the MNIST (LeCun et al. 1998) dataset. Similar to Murphy et al. (2019) and Kalra et al. (2020), we generate sets with 10 instances and use 100k input sets for training, and 10k sets for validation and test. We generate five challenging datasets:

In the *subadditive* MNIST-based **Unique Sum (US)** task (Murphy et al. 2019), the goal is to learn the set function $f_{US}(X) = \sum_{c=0}^{9} c \cdot \mathbb{1}_X(c)$, where $\mathbb{1}_X(c)$ denotes the indicator function. In principle, the mapping from MNIST classes to indexes c is arbitrary. We map each class to the index corresponding to its numerical value, i.e. class '1' is mapped to index $c = 1$, etc. **Weighted Triangular (WTri)** models *superadditive* effects according to $f_{WTri}(X) = \sum_{c=0}^{9} c \cdot T_{count_X(c)}$, where $count_X(c)$ denotes the number of times MNIST image class c appears in set X and T_m is the m-th triangular number, i.e. $T_m = \frac{m \cdot (m+1)}{2}$. **Unique Sum + Synergy Bonus (US+S)** combines both *subadditive and superadditive* effects in a single dataset by computing the label according to

$$ f_{US+S}(X) = \sum_{c=0}^{9} c \cdot \mathbb{1}_X(c) + \sum_{\substack{i=0, j=1 \\ i<j}} 10 \cdot \mathbb{1}_{\{c_i, c_j\}} \in P, \quad (7) $$

where $\mathbb{1}_{\{c_i, c_j\}} \in P$ indicates whether set $\{c_i, c_j\}$ with MNIST classes c_i and c_j appear in a randomly generated set of pairs P.

In addition to tasks based on MNIST, we also generate two datasets based on Fashion-MNIST (Xiao, Rasul, and Vollgraf 2017). In **Unique Count (UC)**, the task is to count the number of uniquely appearing Fashion-MNIST classes. **Triangular Count (TriC)** goes beyond simply counting and computes the set labels according to $f_{TriC}(X) = \sum_{c=0}^{9} T_{count_X(c)}$.

In addition to previously used tasks, we also perform experiments on a real-world **Sentiment Analysis (Sent)** dataset (Pappas and Popescu-Belis 2017). The dataset is based on work by McAuley, Leskovec, and Jurafsky (2012) and available online[2]. A set in this dataset represents a document containing multiple sentences. The goal is to predict the overall sentiment of the documents. We use 300-dimensional feature representation to encode each sentence with a standard library[3] and use the overall sentiment as described in Pappas and Popescu-Belis (2017) as label.

---

[2]Available at https://www.idiap.ch/paper/hatdoc.

[3]Available at github.com/UKPLab/sentence-transformers.
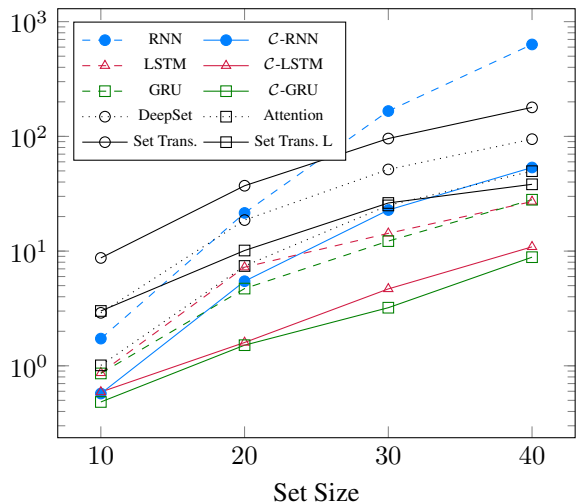
Figure 2: Mean squared error for all architectures and different set sizes in the WTri dataset.

Results

We report the results for all datasets and all architectures in Table 1 and make several key observations. First, Capacity networks achieve overall the best results. $\mathcal{C}$-LSTM and $\mathcal{C}$-GRU perform better than $\mathcal{C}$-RNN, indicating that Capacity networks benefit from a more complex hidden state update approach. Second, and more importantly, Capacity networks perform in almost all cases better than their directly comparable non-capacity counterparts (i.e. RNNs, LSTMs, and GRUs). These results provide clear evidence that the introduced inductive bias has a systematic positive effect on the network performance. Third, datasets US and WTri are easier to learn than US+S and TriC. More difficult tasks (US+S) and more difficult images (TriC) can be explanations for this. Hence, using these datasets in future works will contribute to a better evaluation of neural MIL works. Furthermore, we find that permutation invariant networks do not have a systematic advantage over permutation sensitive models albeit the set functions to learn are permutation invariant. This is an surprising additional insight that can be investigated further in future work.

Experiments with Larger Set Sizes

In Figure 2, we report the performance of all architectures for the WTri task with larger set sizes. These experiments are more challenging and go beyond the scope of prior works such as Murphy et al. (2019) and Kalra et al. (2020) which only consider sets up to 10 instances. Again, we observe that Capacity networks achieve smaller errors that their non-capacity counterpart (dashed vs. solid lines). It should be noted that we use a log scale for the MSE, which means that the performance improvement when using Capacity networks is not approximately constant, but increases substantially with increasing set sizes. We also report the performance of other prior architectures and can confirm that they usually perform worse for larger set sizes.

	US			WTri			US+S		
	30k	50k	70k	30k	50k	70k	30k	50k	70k
RNN	1.42	1.01	1.04	11.68	5.91	3.02	63.87	8.27	7.88
$\mathcal{C}$-RNN (ours)	-0.45	-0.46	-0.54	-6.21	-3.78	-2.11	-53.98	-3.67	-4.81
LSTM	0.84	0.60	0.42	5.05	2.41	1.27	5.71	3.55	2.58
$\mathcal{C}$-LSTM (ours)	**-0.14**	**-0.24**	**-0.12**	-0.73	-0.80	-0.45	+0.43	**-0.80**	**-0.85**
GRU	0.76	0.50	0.40	4.18	1.95	1.01	6.19	4.01	2.82
$\mathcal{C}$-GRU (ours)	±0.00	-0.07	+0.05	**-0.45**	**-0.59**	**-0.35**	**-0.86**	-1.12	-0.88

Table 2: MSE of three Capacity networks and their non-capacity counterparts for different training set sizes. Green and red numbers indicate lower and higher relative MSE with respect to the non-Capacity counterparts, respectively. Best results are highlighted in bold face. Absolute values and results for other architectures can be found in the supplementary material.
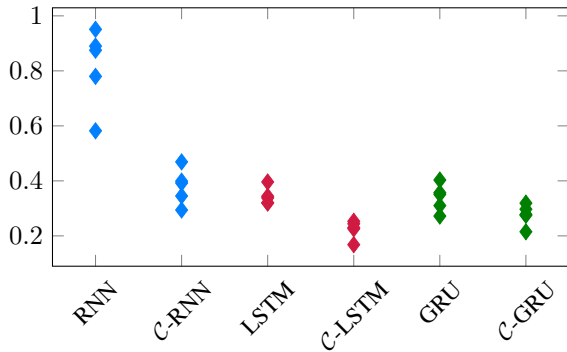
Figure 3: Mean squared error for 5 different random permutations of the instances in the US dataset.

Input	7	8	6	6	3	$\sum$
Expected	7.00	8.00	6.00	0.00	0.00	21.00
$\mathcal{C}$-RNN	6.97	7.99	6.01	0.01	0.00	20.98
Δ	0.03	0.01	0.01	0.01	0.00	0.06
$\mathcal{C}$-LSTM	6.83	7.88	6.03	0.12	0.17	21.03
Δ	0.17	0.12	0.03	0.12	0.17	0.61
$\mathcal{C}$-GRU	6.58	7.47	6.11	0.44	0.40	21.00
Δ	0.42	0.53	0.11	0.44	0.40	1.90

Table 3: Example for improved interpretability in the Unique Sum dataset with 5 instances per set. We show MNIST images (first row), expected intermediate results (second row), predicted intermediate results, and distance to the expected values (Δ rows).

Training with Smaller Amounts of Training Data

In Table 2, we report the performance for different amounts of training data. Similar to the previous experiments, we observe that Capacity networks perform better than their non-capacity counterparts in almost all cases (indicated by green negative numbers). Absolute numbers and results of other models can be found in the supplementary material.

Permutation Sensitivity Evaluation

We perform additional experiments to evaluate how sensitive the sequential architectures are with respect to the order of the input instances. In Figure 3, we plot the results of five different runs with randomly permuted instances. The experiments show that the permutation sensitivity of all models is rather low, except for the RNN. In addition to the results in Table 1, the results show that permutation sensitivity seems to be a minor important issue in these datasets. Moreover, we find that Capacity networks can further reduce the permutation sensitivity for all three base architectures.

Interpretability Experiments

In the following, we demonstrate the improved interpretability of Capacity networks and further advantages of Capacity networks that are related to the improved interpretability.

Improved Interpretability

To evaluate the interpretability of the intermediate results, we extract the intermediate values generated by Capacity networks from the trained models and show which intermediate values are expected. Table 3 illustrates the improved interpretability of Capacity networks in the US dataset. It can be seen that the networks learned the underlying set functions reasonably well. In this example, the $\mathcal{C}$-RNN generates very good intermediate results while the intermediate results generated by the $\mathcal{C}$-GRU are less precise - an insight that cannot be gained by investigating the set-level predictions alone.

Multiplication-based Problem

In general, Capacities and Capacity networks can be applied to any (monotone) non-additive problem, which also includes non-additive problems that have less obvious added values such as multiplication-based problems. To illustrate this, we created a multiplication-based dataset according to $f_{\text{Mult}}(X) = \prod_{i=1}^{n} c_i$, where c_i indicates the class index of instance i and define the empty set to have a utility of 1. Table 4 shows an illustration of the learned intermediate results to demonstrate that the Capacity networks are able to learn added values as expected.

Input	6	5	4	$\sum$
Expected	6.00	24.00	90.00	120.00
$\mathcal{C}$-RNN	5.69	24.49	89.27	119.45
$\mathcal{C}$-LSTM	5.34	25.03	90.34	120.71
$\mathcal{C}$-GRU	2.85	26.21	88.37	117.68

Table 4: Intermediate results in a multiplication-based dataset. In this example, the second added value needs to be 24, since this is the amount that needs to be added to 6 to obtain $6 \cdot 5 = 30$.

	US	WTri	US+S	TriC
$\mathcal{C}$-RNN	**0.29**	0.14	**0.40**	1.32
$\mathcal{C}$-LSTM	1.50	0.09	2.00	**0.57**
$\mathcal{C}$-GRU	2.15	**0.08**	0.47	0.62

Table 5: Quantitative analysis of the generated intermediate results. We report the mean absolute distance to the expected intermediate results.

Evaluation Beyond Input-Output Testing

Capacity networks also allow in-depth evaluation beyond mere input-output testing. More specifically, for Capacity networks, it is not only possible to evaluate if the model produces the correct final outputs, but also to perform a quantitative evaluation of the intermediate results. The results of this evaluation can be found in Table 5. We find that the obtained error for the set labels does not always reliably indicate which model performs best at predicting intermediate results for individual instances. Hence, the quantitative evaluation provides additional insights, which cannot be obtained for encoder-decoder architectures.

Regularizing Latent Intermediate Results

In Figure 4, we demonstrate how prior domain knowledge can be used in Capacity networks by adding additional regularization on the generated intermediate results. To this end, we use the Unique Count problem (Murphy et al. 2019). In this task, we can make use of the prior knowledge that no individual contribution can be larger than 1 by adding a regularization term to the network such that intermediate values larger than 1 are penalized. We find that the added intermediate results regularization improves the training process and leads to better results in fewer iterations and a better performance after training. Adding this kind of regularization is only possible because Capacity networks produce meaningful intermediate results during training and is not possible for their non-Capacity counterparts and other encoder-decoder architectures.

Conclusions

We present Capacity networks, a new family of neural networks to aggregate information from multiple instances. Inspired by non-additive capacities and a sequential decomposition thereof, Capacity networks produce a latent intermediate result for each instance, which models the added
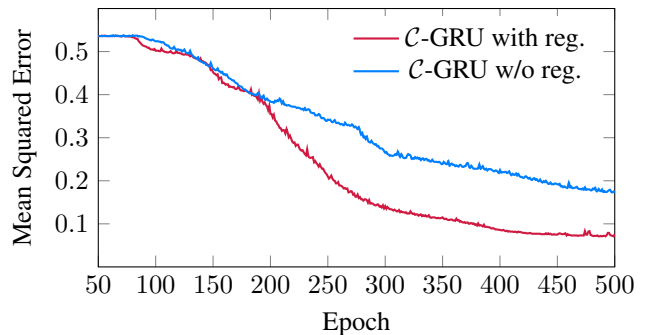
Figure 4: Mean squared test error of two $\mathcal{C}$-GRUs during training. Red and blue lines indicate the learning curves of a $\mathcal{C}$-GRU with regularization and without regularization, respectively.

value of the instance with respect to all already observed instances. This aggregation strategy differs fundamentally from previously used encoder-decoder architectures. Our experiments show that Capacity networks systematically outperform their non-capacity counterparts and other prior architectures, which do not produce intermediate results, in a wide range of setups. Furthermore, we demonstrate the improved interpretability of Capacity networks that allows a detailed inspection of the network internals, an evaluation beyond mere input-output testing, and incorporation of prior knowledge via intermediate result regularization.

Future Work

It is noteworthy that inductive bias presented in this work is not limited to MIL. Aggregating information from multiple sources is also a key problem in areas such as multimodal learning and geometric deep learning. Hence, exploring more application areas beyond MIL for Capacity networks is promising. Furthermore, extending Capacity networks to classification problems is a promising future research direction, especially if the monotonicity constrained is not enforced. Moreover, prior works have shown that learning to order instances can further improve network accuracy (Vinyals, Bengio, and Kudlur 2016). In future research, it would be interesting to see if and to which extent this also applies to Capacity networks.

References

Anderson, D. T.; Grant, J. S.; Islam, M. A.; Murray, B.; and Marcum, R. 2018. Fuzzy Choquet Integration of Deep Convolutional Neural Networks for Remote Sensing. In *Computational Intelligence for Pattern Recognition*, 1–28. Springer International Publishing.

Bahdanau, D.; Cho, K. H.; and Bengio, Y. 2015. Neural Machine Translation by Jointly Learning to Align and Translate. In *Proceeding of the 3rd International Conference on Learning Representations*, 1–15.

Beck, J.; Ciosek, K.; Devlin, S.; Tschiatschek, S.; Zhang, C.; and Hofmann, K. 2020. AMRL: Aggregated Memory For Reinforcement Learning. In *Proceedings of the 8th International Conference on Learning Representations*, 1–14.

Beliakov, G. 2008. Fitting fuzzy measures by linear programming. Programming library fmtools. *IEEE International Conference on Fuzzy Systems*, 862–867.

Carbonneau, M. A.; Cheplygina, V.; Granger, E.; and Gagnon, G. 2018. Multiple instance learning: A survey of problem characteristics and applications. *Pattern Recognition*, 77: 329–353.

Cho, K.; van Merriënboer, B.; Gulcehre, C.; Bahdanau, D.; Bougares, F.; Schwenk, H.; and Bengio, Y. 2014. Learning Phrase Representations using RNN Encoder–Decoder for Statistical Machine Translation. In *Proceedings of the 2014 Conference on Empirical Methods in Natural Language Processing*, 1724–1734.

Choquet, G. 1954. Theory of capacities. *Annales de l'Institut Fourier*, 5: 131–295.

Das, S.; Giles, C. L.; and Sun, G.-Z. 1992. Learning Context-free Grammars: Capabilities and Limitations of a Recurrent Neural Network with an External Stack Memory. In *Proceedings of the 14th Annual Conference of the Cognitive Science Society*, 791–795.

Dias, C. A.; Bueno, J. C. S.; Borges, E. N.; Botelho, S. S. C.; Dimuro, G. P.; ; Lucca, G.; Fernandéz, J.; Bustince, H.; and Drews Junior, P. L. J. 2018. Using the Choquet Integral in the Pooling Layer in Deep Learning Networks. In *Fuzzy Information Processing*, 144–154. Springer International Publishing.

Dietterich, T. G.; Lathrop, R. H.; and Lozano-Pérez, T. 1997. Solving the multiple instance problem with axis-parallel rectangles. *Artificial Intelligence*, 89(1-2): 31–71.

Graves, A.; Wayne, G.; and Danihelka, I. 2014. Neural Turing Machines. In *arXiv preprint*, 1–26.

Herbrich, R.; Minka, T.; and Graepel, T. 2006. TrueSkill: A Bayesian Skill Rating System. In *Advances in Neural Information Processing Systems 20*, 569–576.

Hochreiter, S.; and Schmidhuber, J. 1997. Long Short-Term Memory. *Neural Computation*, 9(8): 1735–1780.

Ilse, M.; Tomczak, J. M.; and Welling, M. 2018. Attention-based deep multiple instance learning. In *Proceedings of the 35th International Conference on Machine Learning*, 3376–3391. ISBN 9781510867963.

Kalra, S.; Adnan, M.; Taylor, G.; and Tizhoosh, H. 2020. Learning Permutation Invariant Representations using Memory Networks. In *Proceedings of the 16th European Conference on Computer Vision*.

Karczmarek, P.; Kiersztyn, A.; and Pedrycz, W. 2018. Generalized Choquet Integral for Face Recognition. *International Journal of Fuzzy Systems*, 20(3): 1047–1055.

Karczmarek, P.; Kiersztyn, A.; and Pedrycz, W. 2019. Generalizations of Aggregation Functions for Face Recognition. In *Artificial Intelligence and Soft Computing*, 182–192.

Kingma, D. P.; and Ba, J. L. 2015. Adam: A method for stochastic optimization. In *Proceedings of the 3rd International Conference on Learning Representations*, 1–15.

LeCun, Y.; Bottou, L.; Bengio, Y.; and Haffner, P. 1998. Gradient-Based Learning Applied to Document Recognition. *Proceedings of the IEEE*, 86(11): 2278–2324.

Lee, J.; Lee, Y.; Kim, J.; Kosiorek, A. R.; Choi, S.; and Teh, Y. W. 2019. Set Transformer: A Framework for Attention-based Permutation-Invariant Neural Networks. In *Proceedings of the 36th International Conference on Machine Learning*, 3744–3753.

Luong, M.-T.; Pham, H.; and Manning, C. D. 2015. Effective Approaches to Attention-based Neural Machine Translation. In *Proceedings of the 2015 Conference on Empirical Methods in Natural Language Processing*, 1412–1421.

Maron, O.; and Lozano-Perez, T. 1998. A framework for multiple-instance learning. *Advances in Neural Information Processing Systems*, 570–576.

McAuley, J.; Leskovec, J.; and Jurafsky, D. 2012. Learning attitudes and attributes from multi-aspect reviews. *Proceedings of the 12th IEEE International Conference on Data Mining*, 1020–1025.

Mena, G.; Belanger, D.; Linderman, S.; and Snoek, J. 2018. Learning Latent Permutations with Gumbel-Sinkhorn Networks.

Meng, C.; Yang, J.; Ribeiro, B.; and Neville, J. 2019. HATS: A hierarchical sequence-attention framework for inductive set-of-sets embeddings. *Proceedings of the ACM SIGKDD International Conference on Knowledge Discovery and Data Mining*, 783–792.

Murphy, R. L.; Srinivasan, B.; Ribeiro, B.; and Rao, V. 2019. Janossy pooling: Learning deep permutation-invariant functions for variable-size inputs. In *Proceedings of the 7th International Conference on Learning Representations*, 1–21.

Niepert, M.; Ahmed, M.; and Kutzkov, K. 2016. Learning Convolutional Neural Networks for Graphs. In *Proceedings of the 33rd International Conference on Machine Learning*, 2014–2023.

Pappas, N.; and Popescu-Belis, A. 2017. Explicit document modeling through weighted multiple-instance learning. *Journal of Artificial Intelligence Research*, 58: 591–626.

Qi, C. R.; Su, H.; Mo, K.; and Guibas, L. J. 2017. PointNet: Deep learning on point sets for 3D classification and segmentation. *Proceedings of the IEEE Conference on Computer Vision and Pattern Recognition*, 77–85.

Ray, S.; and Page, D. 2001. Multiple Instance Regression. In *Proceedings of the International Conference on Machine Learning*, 425 – 432.

Schmidhuber, J. 1992. Learning to Control Fast-weight Memories: an Alternative to Dynamic Recurrent Networks. *Neural Computation*, 4(1): 131–139.

Schmidhuber, J. 1993. A 'Self-Referential' Weight Matrix. In *Proceedings of the International Conference on Artificial Neural Networks*, 446–450.

Schmidt, R. M.; Schneider, F.; and Hennig, P. 2020. Descending through a Crowded Valley - Benchmarking Deep Learning Optimizers. In *arXiv*, 1–30.

Scott, G. J.; Marcum, R. A.; Davis, C. H.; and Nivin, T. W. 2017. Fusion of Deep Convolutional Neural Networks for Land Cover Classification of High-Resolution Imagery. *IEEE Geoscience and Remote Sensing Letters*, 14(9): 1638–1642.

Segol, N.; and Lipman, Y. 2020. On Universal Equivariant Set Networks. In *Proceedings of the 8th International Conference on Learning Representations*.

Shi, Y.; Oliva, J.; and Niethammer, M. 2020. Deep Message Passing on Sets. In *Proceedings of the 34th AAAI Conference on Artificial Intelligence*, 5750–5757.

Soelch, M.; Akhundov, A.; van der Smagt, P.; and Bayer, J. 2019. On Deep Set Learning and the Choice of Aggregations. In *Proceeding of the 28th International Conference on Artificial Neural Networks*, 444–457. Springer International Publishing.

Sudharshana, P. J.; Petitjean, C.; Spanhol, F.; Oliveira, L.; Honeine, P.; Sudharshana, P. J.; Petitjean, C.; Spanhol, F.; Oliveira, L.; and Heutte, L. 2019. Multiple Instance Learning for Histopathological Breast Cancer Images. *Expert Systems with Applications*, 117: 103–111.

Sugeno, M. 1974. *Theory of fuzzy integrals and its applications*. Ph.d. thesis, Tokyo Institute of Technology.

Tehrani, A. F.; Cheng, W.; Dembczyński, K.; and Hüllermeier, E. 2012. Learning monotone nonlinear models using the Choquet integral. *Machine Learning*, 89(1-2): 183–211.

Tehrani, A. F.; Cheng, W.; and Hullermeier, E. 2012. Preference learning using the choquet integral: The case of multipartite ranking. *IEEE Transactions on Fuzzy Systems*, 20(6): 1102–1113.

Vaswani, A.; Shazeer, N.; Parmar, N.; Uszkoreit, J.; Jones, L.; Gomez, A. N.; Kaiser, L.; and Polosukhin, I. 2017. Attention Is All You Need. In *Advances in Neural Information Processing Systems 30*, 6000–6010.

Vinyals, O.; Bengio, S.; and Kudlur, M. 2016. Order matters: Sequence to sequence for sets. In *Proceeding of the 4th International Conference on Learning Representations*, 1–11.

Weston, J.; Chopra, S.; and Bordes, A. 2015. Memory Networks. In *Proceeding of the 3rd International Conference on Learning Representations*, 1–15.

Xiao, H.; Rasul, K.; and Vollgraf, R. 2017. Fashion-MNIST: A novel image dataset for benchmarking machine learning algorithms. In *arXiv preprint*, 1–6.

Yang, B.; Wang, S.; Markham, A.; and Trigoni, N. 2020. Robust Attentional Aggregation of Deep Feature Sets for Multi-view 3D Reconstruction. *International Journal of Computer Vision*, 128(1): 53–73.

Zaheer, M.; Kottur, S.; Ravanbakhsh, S.; Poczos, B.; Salakhutdinov, R.; and Smola, A. 2017. Deep Sets. In *Proceeding of the 31st Conference on Neural Information Processing Systems*, 1–11.

Zhang, Y.; Hare, J.; and Prügel-Bennett, A. 2020. FSPool: Learning Set Representations with Featurewise Sort Pooling. In *Proceedings of the 8th International Conference on Learning Representations*.

Zhang, Y.; Prügel-Bennett, A.; and Hare, J. 2019. Learning Representations of Sets through Optimized Permutations. In *Proceeding of the 7th International Conference on Learning Representations*, 1–15.

Supplementary Material

In the supplementary material, we provide additional information on implementation details, model sizes, and the hyperparameter optimization. Furthermore, we provide additional results for experiments in the main paper and generate and evaluate potential intermediate results of non-Capacity networks.

Implementation Details

In the following, we provide additional information on the different architectures used in the experiments. As already described in the main paper, the architectures can be described in terms of encoder and decoder modules. Different conventions are used to label different parts of the networks. In particular, the pooling operation used in parallel networks can be viewed as part of the encoder or as additional module. As a consequence, these networks have also been described as encoder-pooling-decoder networks (Lee et al. 2019). In this work, we consider the pooling layer as part of the encoder, since the pooling generates a joint representation of all input instances, a task that belongs to the domain of encoders. Similar to Zaheer et al. (2017), we performed initial experiments with 2 and 3 layer fully connected networks for the encoder and decoder modules (see Appendix for more information). However, using more complex networks is possible and perhaps beneficial for more complex input data. We denote the fully connected layers in the encoder and decoder by ϵ ('epsilon' for 'encoder') and δ ('delta' for 'decoder'), respectively. Furthermore, we note that the networks only use one instantiation of ϵ and δ. Hence, different applications of ϵ and δ in the architectures share parameters with all other applications.

All models use ReLu activation in the encoders and decoders. We have also performed initial experiments with Sigmoid and Tanh activation functions. However, we observed that ReLu often performs better in terms of mean squared error and results in a more stable training process. ReLu activations have also been used by prior works (Zaheer et al. 2017).

In non-Capacity networks, we denote the set representation by Z, whereas in Capacity networks, we denote the representation used to generate the intermediate outputs by z_i. All models use the same number of dimensions for internal representation (i.e. $|Z| = |z_i|$). Having the same number of dimensions further improves the comparability of the models, since the performance differences between the models cannot be explained by different hidden dimension sizes.

In the following, we describe further architecture-specific details.

DeepSet

$$Z = \mathsf{encoder}(X) = \sum_{x \in X} \epsilon(x)$$
$$Y = \mathsf{decoder}(Z) = \delta(Z) \tag{8}$$

Attention

$$Z = \mathsf{encoder}(X) = \sum_{x \in X} a_i \cdot \epsilon(x_i)$$
$$a_i = \frac{\exp h(x_i)}{\sum_{j=1}^{|X|} \exp h(x_j)} \tag{9}$$
$$h(x) = B \cdot \tanh(A \cdot x + a) + b,$$
$$A \in \mathbb{R}^{n \times d}, B \in \mathbb{R}^{1 \times n}, a \in \mathbb{R}^n, b \in \mathbb{R}$$
$$Y = \mathsf{decoder}(Z) = \delta(Z)$$

RNN

$$Z = \mathsf{encoder}(X) = h_n$$
$$h_i = \tanh(A \cdot [h_{i-1}, x_i] + a),$$
$$A \in \mathbb{R}^{2n \times d}, a \in \mathbb{R}^d \tag{10}$$
$$Y = \mathsf{decoder}(Z) = \delta(Z)$$

where $[\cdot, \cdot]$ denotes concatenation of two vectors, d equals the number of hidden dimensions, and $h_0 = \vec{0}$ is used as initial hidden state.

LSTM

$$Z = \mathsf{encoder}(X) = \mathrm{LSTM}_i$$
$$Y = \mathsf{decoder}(Z) = \delta(Z) \tag{11}$$

where LSTM_i is an LSTM cell according to Hochreiter and Schmidhuber (1997) and $c_0 = \vec{0}$ is used as initial cell state.

GRU

$$Z = \mathsf{encoder}(X) = \mathrm{GRU}_i$$
$$Y = \mathsf{decoder}(Z) = \delta(Z) \tag{12}$$

where GRU_i is a GRU cell according to Cho et al. (2014) and $c_0 = \vec{0}$ is used as initial cell state.

$\mathcal{C}$-RNN

$$z_i = \mathsf{encoder}(x_i) = h_i$$
$$h_i = \tanh(A \cdot [h_{i-1}, x_i] + a),$$
$$A \in \mathbb{R}^{2n \times d}, a \in \mathbb{R}^d, h_0 = \vec{0}$$
$$y_i = \mathsf{decoder}(z_i) = \delta(z_i) \tag{13}$$
$$Y = \sum_{i=0}^{|X|} y_i$$

$\mathcal{C}$-LSTM

$$z_i = \mathsf{encoder}(x_i) = \mathrm{LSTM}_i$$
$$y_i = \mathsf{decoder}(z_i) = \delta(z_i)$$
$$Y = \sum_{i=0}^{|X|} y_i \tag{14}$$

$\mathcal{C}$-GRU

$$z_i = \mathsf{encoder}(x_i) = \mathrm{GRU}_i$$
$$y_i = \mathsf{decoder}(z_i) = \delta(z_i)$$
$$Y = \sum_{i=0}^{|X|} y_i \tag{15}$$

Furthermore, we refer to Lee et al. (2019) and to http://github.com/juho-lee/set_transformer for a detailed description and implementation of the Set Transformer architecture.

Model Sizes

Table 6 shows the number of trainable parameters for each model. Most important, all sequential models (i.e. RNN, LSTM, and GRU) and their Capacity Network counterparts (i.e. $\mathcal{C}$-RNN, $\mathcal{C}$-LSTM, and $\mathcal{C}$-GRU) have the same number of parameters. Hence, the performance differences observed in the experiments cannot be explained by different model sizes.

Architecture	Parameters
DeepSet	13,601
Attention	17,794
Set Trans.	15,809
Set Trans. L	34,753
RNN	15,681
LSTM	22,049
GRU	19,937
$\mathcal{C}$-RNN (ours)	15,681
$\mathcal{C}$-LSTM (ours)	22,049
$\mathcal{C}$-GRU (ours)	19,937

Table 6: Number of trainable parameters for instance embedding size of 64 and latent representation dimension of 32.

Hyperparameter Optimization

We performed a hyperparameter search for the following parameters and ranges: learning rate $\in \{0.01, 0.001, 0.0001\}$, number of hidden dimensions $\in \{8, 16, 32\}$, number of fully connected layers for encoders and decoders $\in \{2, 3\}$. In total, we performed 486 experiments for 10 architectures and 3 datasets. Table 10 shows the results of the hyperparameter optimization. It can be seen that all architectures perform better with 3 instead of 2 fully connected layers for the encoder and decoder sub-networks. Moreover, 32 dimensional latent representations work best for most networks. The only exception are $\mathcal{C}$-GRUs, for which 16 dimensions work equally well. Furthermore, a learning rate of 0.001 leads to best results for all networks. Learning rates of 0.01 and 0.0001 lead to good results in only 2 out of 30 setups. To sum, we find a common trend for all networks and use a learning rate of 0.001, 32 hidden dimensions, and 3 fully connected layers in all experiments. Furthermore, we performed experiments with different batch sizes in the range of 100, 500, 1000, and 2000 and found that a batch size of 1000 works well in general.

Dataset Statistics

In this section, we report statistics of the generated datasets. Table 7 shows mean, median, variance, and standard deviation of several datasets. Figure 5 illustrates the distribution of set utilities for the datasets US, WTri, and US+S.

Additional Experimental Results for Table 1

Table 8 and Table 9 provide further details for the experiments in Table 1. We report median and standard deviation

Dataset	Set Size	Mean	Med	Variance	StDev
US	10	29.34	30	39.88	6.32
WTri	10	65.19	62	407.16	20.18
US+S	10	49.80	50	169.87	13.03
TriC	10	14.50	14	4.02	2.00
WTri	20	175.42	170.0	1869.67	43.24
WTri	30	330.77	323.0	4885.71	69.9
WTri	40	530.93	521.0	9805.65	99.02
US	var.	28.58	29	60.73	7.79
WTri	var.	66.84	62	1068.33	32.69
US+S	var.	50.56	50	292.40	17.10
TriC	var.	32.11	29	108.26	10.40

Table 7: Mean, median (Med), variance, and standard deviation (StDev) of generated datasets with fixed and varying set sizes.

to allow a better interpretation of the reported results.

	US	WTri	US+S	TriC
RNN	0.91	1.65	7.04	4.09
LSTM	0.41	0.87	2.80	**1.01**
GRU	0.48	0.89	2.56	3.98
$\mathcal{C}$-RNN (ours)	0.44	0.61	2.61	4.08
$\mathcal{C}$-LSTM (ours)	0.27	0.56	**1.62**	**1.01**
$\mathcal{C}$-GRU (ours)	0.27	**0.48**	1.93	1.26
DeepSet	**0.24**	2.87	2.43	1.02
Attention	0.53	0.94	3.01	4.08
Set Trans.	1.93	8.39	15.15	1.21
Set Trans. L	1.66	2.80	11.31	1.19

Table 8: Median of the results in Table 1.

	US	WTri	US+S	TriC
RNN	0.10	0.21	0.64	0.00
LSTM	0.03	0.21	0.18	0.01
GRU	0.04	0.24	0.29	1.44
$\mathcal{C}$-RNN (ours)	0.03	0.07	0.21	1.30
$\mathcal{C}$-LSTM (ours)	0.01	0.13	0.03	0.02
$\mathcal{C}$-GRU (ours)	0.06	0.08	0.49	1.39
DeepSet	0.06	0.15	0.52	1.47
Attention	0.20	0.21	0.96	1.36
Set Trans.	0.09	1.44	1.25	0.02
Set Trans. L	0.11	0.61	2.47	0.02

Table 9: Standard deviation (StDev) for the experiments in Table 1.

Network	E/D	ND	LR=	US 0.01	US 0.001	US 0.0001	WTri 0.01	WTri 0.001	WTri 0.0001	US+S 0.01	US+S 0.001	US+S 0.0001
DeepSet	2fc	8		10.53	4.90	10.45	40.09	33.65	101.69	111.83	43.50	112.10
		16		6.43	2.73	3.35	19.06	22.66	52.38	52.13	16.07	29.37
		32		2.35	2.19	3.10	19.80	19.15	27.72	15.31	14.14	18.34
	3fc	8		13.12	3.11	3.84	7.94	11.23	26.10	157.40	-	88.05
		16		0.39	0.30	3.80	**2.97**	5.19	15.30	5.56	-	29.25
		32		0.53	**0.27**	0.94	3.20	3.60	11.86	8.68	**2.79**	7.16
Attention	2fc	8		-	7.20	9.54	-	28.08	52.37	-	40.34	78.56
		16		-	0.88	2.89	-	5.43	12.72	-	6.38	37.33
		32		-	0.52	1.25	-	3.76	7.95	-	3.60	11.97
	3fc	8		-	-	-	-	-	-	-	-	-
		16		-	**0.21**	1.77	-	2.16	5.93	-	3.80	44.75
		32		-	0.22	0.46	-	**0.98**	4.12	-	**1.77**	28.30
$\mathcal{C}$-RNN	2fc	8		-	5.63	10.49	-	36.61	54.72	-	83.70	90.56
		16		-	1.38	4.16	-	5.42	26.88	-	18.34	63.88
		32		-	0.80	1.63	-	2.60	10.22	-	6.58	15.37
	3fc	8		-	4.21	8.59	-	25.26	36.73	-	74.67	91.49
		16		-	0.48	2.43	-	1.93	14.38	-	13.47	53.18
		32		-	**0.47**	0.79	-	**0.57**	6.48	-	**2.86**	11.99
$\mathcal{C}$-LSTM	2fc	8		-	1.39	2.97	14.09	12.09	27.01	-	31.68	67.64
		16		-	0.48	1.41	-	5.10	14.16	-	3.02	7.97
		32		-	0.44	0.92	-	2.38	8.21	-	2.65	5.52
	3fc	8		-	2.22	3.95	-	5.82	22.62	-	26.34	53.95
		16		-	**0.20**	1.38	39.67	1.12	13.08	-	1.73	8.24
		32		-	0.23	0.50	-	**0.52**	5.02	-	**1.04**	3.80
$\mathcal{C}$-GRU	2fc	8		-	1.53	3.86	-	15.67	28.21	-	29.71	66.70
		16		-	0.58	1.25	-	3.59	11.17	-	3.99	8.05
		32		-	0.47	0.63	-	3.40	8.37	-	3.18	4.87
	3fc	8		-	1.47	2.04	-	9.84	20.02	-	20.28	37.06
		16		-	**0.29**	0.71	-	0.84	7.32	-	**1.39**	4.85
		32		-	**0.29**	0.50	-	**0.38**	4.05	-	1.46	2.83
RNN	2fc	8		-	2.55	16.48	-	38.75	111.25	-	44.47	113.77
		16		-	2.10	3.60	-	15.21	64.85	-	12.89	57.02
		32		-	1.75	1.99	-	5.98	23.85	-	12.10	12.28
	3fc	8		-	-	-	-	-	-	-	-	-
		16		-	**0.75**	2.50	-	9.97	56.01	-	5.28	45.47
		32		-	1.06	0.76	-	**1.88**	15.88	-	5.95	**4.40**
LSTM	2fc	8		-	0.83	2.34	-	12.32	44.67	-	16.23	32.87
		16		-	0.60	0.77	-	3.85	17.51	-	3.87	4.98
		32		-	0.57	0.94	-	3.55	9.21	-	3.09	6.78
	3fc	8		-	-	-	-	7.23	-	-	-	-
		16		-	0.44	0.50	-	2.05	15.69	-	**2.25**	3.22
		32		-	**0.31**	0.57	-	**0.74**	5.10	-	2.27	2.98
GRU	2fc	8		-	0.71	1.43	-	11.22	26.02	-	12.66	20.74
		16		-	0.61	0.74	-	4.46	13.94	-	3.23	4.37
		32		-	0.52	0.60	-	2.26	8.75	-	2.82	3.19
	3fc	8		-	-	-	50.76	-	-	-	-	-
		16		-	0.48	0.53	-	2.11	7.46	-	**2.49**	3.19
		32		-	**0.38**	0.54	-	**0.65**	4.25	-	2.57	2.67
Set Trans.		8		4.29	3.43	4.95	33.80	27.07	50.27	25.24	20.54	25.74
		16		2.08	2.69	3.79	18.62	16.62	27.55	21.58	16.99	19.68
		32		2.89	**1.91**	2.73	28.89	**8.40**	22.12	16.07	**11.98**	14.34
Set Trans. L		8		2.68	2.42	3.08	15.45	17.19	35.02	16.44	**18.22**	19.41
		16		1.85	1.99	2.54	17.09	8.00	27.06	13.53	12.69	13.41
		32		2.20	**1.79**	2.12	25.81	**2.38**	13.51	13.19	12.40	13.26

Table 10: Hyperparameter search results. We report mean squared validation error for all architectures, used encoder/decoder sub-networks (E/D), number of hidden dimensions (ND), and learning rate (LR) for three datasets. For Set Trans. and Set Trans. L, we use the architecture used in prior work (Lee et al. 2019) and, hence, do not use different encoder/decoder sub-networks. Cells without result indicate that the network did not converge to a reasonable result in this setup. We highlight the best result in each box.
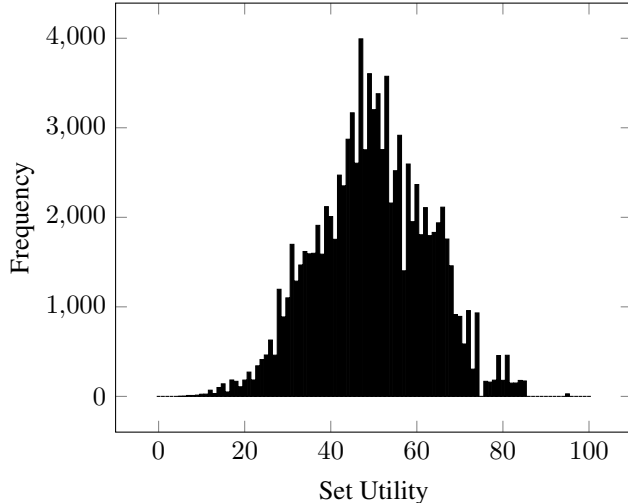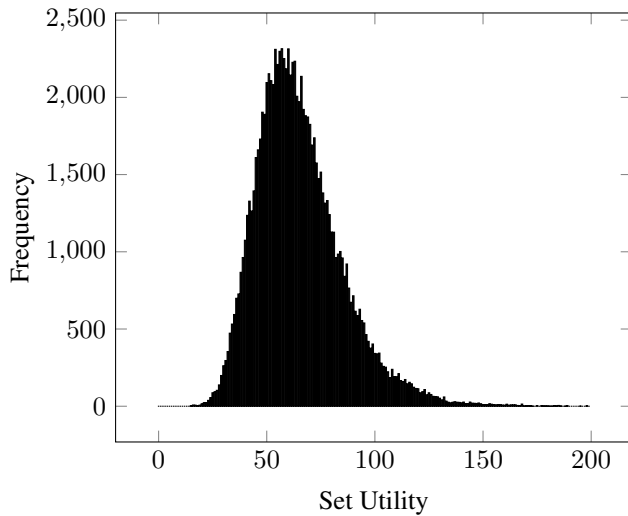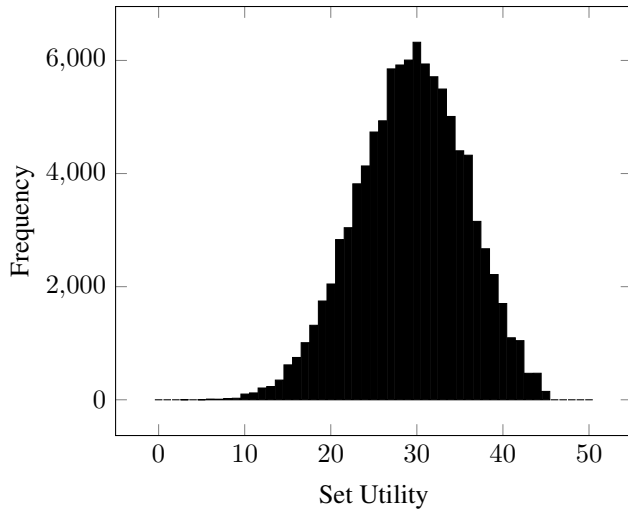
Figure 5: Distribution of set utilities for different datasets. Top: US, middle: WTri, bottom: US+S

Results without Enforcing Non-negative Intermediate Results

In Table 11, we report results without enforcing non-negative intermediate results by removing abs(.) in Equation 8. We observe that the accuracy can further improve in several cases and that we achieve even new best results in three datasets (US, US+S, TriC). These results indicate that removing the monotonicity constraint can be helpful to achieve better results. However, it should be considered Choquet capacities always enforce monotonicity. Hence, by removing the monotonicity constraint the proposed idea becomes less strongly related to Choquet capacities.

	US	WTri	US+S	TriC
$\mathcal{C}$-RNN (w/o abs.)	0.40	0.79	2.12	**0.98**
$\mathcal{C}$-LSTM (w/o abs.)	0.22	0.66	1.28	1.03
$\mathcal{C}$-GRU (w/o abs.)	**0.21**	0.75	**1.05**	1.02

Table 11: Results without absolute value computation.

Additional Results for Varying Set Sizes

To evaluate the sensitivity of the models to varying set sizes, we generated a dataset with $6, 8, 10, 12$, and 14 instances. In addition to Table 12, we report the median of the mean squared error for experiments with varying set sizes in Table 13. The results confirm previously made observations that Capacity networks perform better than their non-Capacity counterparts in these experiments.

	US	WTri	US+S	TriC
RNN	1.31	3.55	9.12	107.51
LSTM	0.42	2.14	2.76	2.16
GRU	0.43	1.01	2.45	105.26
$\mathcal{C}$-RNN	0.36	0.98	2.92	38.07
$\mathcal{C}$-LSTM	**0.25**	0.77	**1.56**	1.89
$\mathcal{C}$-GRU	0.29	**0.40**	1.75	**1.57**

Table 12: Mean squared errors for varying set sizes.

	US	WTri	US+S	TriC
RNN	1.20	4.06	9.51	107.51
LSTM	0.40	1.59	2.77	2.11
GRU	0.40	0.98	2.56	105.26
$\mathcal{C}$-RNN	0.39	1.03	3.01	3.44
$\mathcal{C}$-LSTM	**0.26**	0.69	**1.52**	1.82
$\mathcal{C}$-GRU	0.28	**0.40**	1.78	**1.49**

Table 13: Median for experiments with varying set sizes.

Additional Results for Experiments with Varying Amounts of Training Data

Table 14 contains results for parallel architectures for the experiments with varying amounts of training data. In contrast

	US			WTri			US+S		
	30k	50k	70k	30k	50k	70k	30k	50k	70k
DeepSet	1.54	9.84	0.35	10.85	6.20	4.24	111.38	6.03	55.68
Attention	1.88	0.42	0.35	5.56	2.70	2.18	65.61	4.42	2.24
Set Trans.	4.61	3.30	2.50	34.03	19.08	12.53	27.07	20.39	17.28
Set Trans. L	3.50	2.62	1.95	20.81	13.47	9.36	18.63	17.17	14.97
RNN	1.42	1.01	1.04	11.68	5.91	3.02	63.87	8.27	7.88
LSTM	0.84	0.60	0.42	5.05	2.41	1.27	5.71	3.55	2.58
GRU	0.76	0.50	0.40	4.18	1.95	1.01	6.19	4.01	2.82
$\mathcal{C}$-RNN	0.98	0.55	0.50	5.47	2.14	0.91	9.89	4.60	3.07
$\mathcal{C}$-LSTM	**0.70**	**0.37**	**0.29**	4.33	1.60	0.82	**6.14**	**2.75**	**1.73**
$\mathcal{C}$-GRU	0.76	0.42	0.45	**3.73**	**1.37**	**0.66**	5.33	2.89	1.94

Table 14: Mean squared error of three architecture vs. each architecture equipped with our newly proposed inductive bias on three datasets with different non-additive utility functions for four different training set sizes.

to the main paper, in which we focused on the difference between Capacity networks and their non-Capacity counterparts by showing relative values, we new report absolute values.

Quantitative Results for Figure 3

In Table 15, we report the quantitative results for the illustration in Figure 3.

	RNN	$\mathcal{C}$-RNN	LSTM	$\mathcal{C}$-LSTM	GRU	$\mathcal{C}$-GRU
Median	0.88	**0.39**	0.34	**0.23**	0.35	**0.28**
Mean	0.82	**0.38**	0.34	**0.22**	0.34	**0.28**
StDev	0.13	**0.06**	**0.03**	**0.03**	0.05	**0.04**

Table 15: Median, mean, and standard deviation (StDev) for the results in Figure 3.

Additional Improved Interpretability Illustrations

Table 16 provides more insights on learned intermediate results similar to Table 3. Specifically, we provide two more examples for the WTri and the US+S dataset. Similar to the results in Table 3, it can be observed that Capacity networks learn reasonable intermediate results without any instance-level supervision.

Evaluating Intermediate Results of Non-Capacity Networks

In principle, it is possible to obtain results similar to the intermediate results generated by Capacity networks by applying non-Capacity networks to subsets of the input. To this end, we train the networks as described previously an apply the decoder of the networks to the subsets $\{x_1\}, \{x_1, x_2\}, \ldots$. The added valued of x_i can then be computed according to decoder($\{x_1, \ldots, x_i\}$) − decoder($\{x_1, \ldots, x_{i-1}\}$). However, unlike Capacity networks, the decoder of non-Capacity networks has never been

Input						$\sum$
Expected	2.00	4.00	3.00	6.00	6.00	21.00
$\mathcal{C}$-RNN	1.99	4.00	2.98	5.95	5.65	20.57
Δ	0.01	0.00	0.02	0.05	0.35	0.43
$\mathcal{C}$-LSTM	2.02	3.97	3.04	6.00	6.21	21.24
Δ	0.02	0.03	0.04	0.00	0.21	0.30
$\mathcal{C}$-GRU	2.03	3.97	2.92	5.95	6.38	21.25
Δ	0.03	0.03	0.08	0.05	0.38	0.57

Input						$\sum$
Expected	7.00	9.00	12.00	0.00	5.00	33.00
$\mathcal{C}$-RNN	6.86	8.97	11.92	0.11	5.03	32.89
Δ	0.14	0.03	0.08	0.11	0.03	0.39
$\mathcal{C}$-LSTM	6.09	8.50	12.27	0.57	5.70	33.13
Δ	0.91	0.50	0.27	0.57	0.70	2.95
$\mathcal{C}$-GRU	6.81	8.59	11.91	0.24	5.01	32.56
Δ	0.19	0.41	0.09	0.24	0.01	0.94

Table 16: Illustration of improved interpretability in the WTri (top) and US+S (bottom) dataset. We show the MNIST input instances (first row), the expected intermediate results (second row), the predicted intermediate results, and the difference to the expected value (Δ rows).

trained to generate good intermediate results during training. Hence, it is unlikely that this strategy performs well. To demonstrate this, we apply the idea to the WTri and TriC datasets and compute the mean absolute error of the obtained intermediate results with respect to the expected intermediate results. Table 18 shows that non-Capacity indeed generate very poor intermediate results, specifically in the WTri dataset, compared to Capacity networks.

Accuracy Results for Table 2

In Table 17, we report the accuracy results for the RNN and the $\mathcal{C}$-RNN architecture. The results show that not only

	US			WTri			US+S		
	30k	50k	70k	30k	50k	70k	30k	50k	70k
RNN	60.61	68.93	73.22	17.01	29.06	40.13	**46.70**	54.52	53.71
$\mathcal{C}$-RNN	**71.42**	**92.31**	**96.13**	**33.04**	**71.37**	**74.30**	30.67	**58.74**	**76.51**

Table 17: Additional accuracy results for Table 2.

	RNN	$\mathcal{C}$-RNN	LSTM	$\mathcal{C}$-LSTM	GRU	$\mathcal{C}$-GRU
WTri	12.45	**0.12**	17.56	**0.11**	13.25	**0.09**
TriC	3.84	**1.10**	3.47	**0.81**	11.75	**1.15**

Table 18: Mean absolute error of intermediate results.

the mean squared error improves substantially, but also the achieved accuracy if the task is understood as classification problem. It is likely that better results can be achieved if a classification loss such as the cross-entropy loss are used if the accuracy should be maximized.